Talanta 129 (2014) 143–149

Contents lists available at ScienceDirect

Talanta

journal homepage: www.elsevier.com/locate/talanta

Evaluation of transformer insulating oil quality using NIR, fluorescence, and NMR spectroscopic data fusion

Mariana S. Godinho [a], Marcos R. Blanco [b], Francisco F. Gambarra Neto [a], Luciano M. Lião [a], Marcelo M. Sena [c], Romà Tauler [d], Anselmo E. de Oliveira [a,*]

[a] Universidade Federal de Goiás, PO Box 131, 74001-970 Goiânia, GO, Brazil
[b] DO-DPEM, CELG D, 74805-180 Goiânia, GO, Brazil
[c] Departamento de Química, ICEx, Universidade Federal de Minas Gerais, Belo Horizonte, MG, Brazil
[d] Department of Environmental Chemistry, IDAEA-CSIC, Barcelona, Spain

ARTICLE INFO

Article history:
Received 9 December 2013
Received in revised form
14 May 2014
Accepted 16 May 2014
Available online 27 May 2014

Keywords:
Data fusion
Power transformer
Mineral insulating oil
NIR
Spectrofluorimetry
NMR
PLS
VIP

ABSTRACT

Power transformers are essential components in electrical energy distribution. One of their most important parts is the insulation system, consisting of Kraft paper immersed in insulating oil. Interfacial tension and color are major parameters used for assessing oil quality and the system's degradation. This work proposes the use of near infrared (NIR), molecular fluorescence, and ^{1}H nuclear magnetic resonance (NMR) spectroscopy methods combined with chemometric multivariate calibration methods (Partial Least Squares – PLS) to predict interfacial tension and color in insulating mineral oil samples. Interfacial tension and color were also determined using tensiometry and colorimetry as standard reference methods, respectively. The best PLS model was obtained when NIR, fluorescence, and NMR data were combined (data fusion), demonstrating synergy among them. An optimal PLS model was calculated using the selected group of variables according to their importance on PLS projections (VIP). The root mean square errors of prediction (RMSEP) values of 2.9 mN m^{-1} and 0.3 were estimated for interfacial tension and color, respectively. Mean relative standard deviations of 1.5% for interfacial tension and 6% for color were registered, meeting quality control requirements set by electrical energy companies. The methods proposed in this work are rapid and simple, showing great advantages over traditional approaches, which are slow and environmentally unfriendly due to chemical waste generation.

1. Introduction

Electricity transmission and distribution require the use of high-voltage power transformers. These devices have an insulation system which consists of Kraft paper immersed in insulating mineral oil [1]. Kraft paper is composed of cellulose, hemicelluloses, and lignin [2]. The gradual depolymerization of Kraft paper inside a power transformer releases its degradation products into the insulating oil. Cellulose degradation involves breaking glycosidic bonds that hold glucose rings together [3]. During the decomposition reaction of cellulose chains, water and furanic compounds such as 2-furaldehyde, 5-hydroxymethyl-2-furaldehyde, 5-methyl-2-furaldehyde, and furfurylalcohol are generated [4]. These compounds change the oil's physicochemical properties, such as color and interfacial tension. The latter, which measures the interfacial force required to separate insulating oil and water, is one of the most important parameters used for evaluating the degradation of the insulation system. It corresponds to an indirect measurement of polar substances, such as furanic compounds and water, so the more degraded the insulating system, the lower the interfacial tension [5,6]. Color is important when assessed together with other parameters. It is determined by a colorimeter and represented by a number (between 0.5 and 8, measured at 0.5 increments), which is compared to ASTM D1500-12 color standards [7] to assess whether or not the oil is degraded. Color increases along with the insulation system's degradation and has a reasonable correlation with interfacial tension.

Different analytical techniques are used to quantify gaseous and furanic compounds, as well as physicochemical analyses. Dissolved gas analysis (DGA), degree of polymerization (DP) [8,9], and HPLC analysis of furans [10] have been commonly used to assess the degradation of paper oil's insulation system. All these techniques pose some drawbacks, e.g. destructive, time-consuming, and relatively costly analysis, sample pretreatment demand, solvent consumption, and waste generation. On the other hand, spectroscopic techniques such as molecular fluorescence and

* Corresponding author.
E-mail address: elcana@ufg.br (A.E. de Oliveira).

http://dx.doi.org/10.1016/j.talanta.2014.05.021
0039-9140/

FT-NIR are fast, non-destructive, non-invasive, and low-cost. Despite being an expensive technique, NMR spectroscopy presents the advantage of generating a small amount of chemical waste. Partial Least Squares (PLS) chemometric methods combined with spectroscopic techniques have been proposed for the quantitative analysis of physicochemical parameters from spectroscopic measures in different applied fields and problems (see, for instance, [6,11,12]).

This study offers a simple, rapid, and non-destructive method to determine interfacial tension and color parameters of real insulating oil samples collected from the power industry via FT-NIR, ^{1}H NMR, and molecular fluorescence combined with PLS. The synergy among spectroscopy techniques is also evaluated by data fusion. Analysis results are reported and discussed in different sections of this paper.

2. Materials and methods

2.1. Data fusion and VIP scores

Data fusion merges the information provided by several analytical instruments or sensors and allows a large number of various multivariate signals to be handled, thus requiring the use of chemometric tools. Compilation of data from different non-specific techniques provides complementary interpretations and facilitates full product description [13]. For each sample, all spectral variables from different instrument types and sources are concatenated into a single vector, known as meta-spectrum.

Since the late 1980s, data fusion has been applied in fields like engineering and robotics [14]. In recent years, it has been used in analytical chemistry to develop classification and multivariate calibration models, mainly in the analysis of complex food sample matrices, such as olive oil [15–17], beer [13], wine [18], dye [19], and meat [20], but also as regards other sample matrices, such as pigment determination in works of art [21]. The most often used spectroscopic techniques have been UV–Visible, infrared (NIR and MIR), Raman, fluorescence, and mass spectrometry. Data fusion can be classified in three levels: low, medium, and high [22]. Low-level fusion consists in directly combining original signals (spectra) after preprocessing steps. Medium-level fusion involves the extraction of features or selection of variables before data fusion. Finally, in high-level fusion, a multivariate model is built separately for each technique and individual outputs are combined to produce a final result [23]. The present work employed the most common low-level data fusion. Fluorescence excitation-emission spectral data matrices (EEM), NIR, and NMR spectra were fused after specific preprocessing steps. Following data fusion, a strategy of data compression and variable selection based on variable importance in projection (VIP) scores obtained by PLS regression [24] was used.

VIP scores, whose performance has recently been evaluated [25], measure the importance of each variable in the projection used by a particular PLS model via the coefficients of a variable in every component, together with the significance of each component in regression. Subsequently, they can also be used for variable selection, and the criterion for the selection of variable j is the average of squared VIP scores being greater than or equal to 1. The importance of the j-th predictor variable based on a model with h LVs can be calculated by

$$VIP_j = \sqrt{\frac{J}{\sum_h SS(b_h t_h)} \sum_h w_{hj}^2 SS(b_h t_h)}$$

where J is the number of predictor variables, w_{hj} is the loading weight of the j-th predictor variable in the h-th PLS factor, and $SS(b_h t_h)$ is the percentage of y explained by the h-th LV [26]. Reference [27] provides more details of the PLS method.

2.2. Insulating oil sampling and reference methods

One hundred mineral insulating oil samples from power transformers of CELG D, the electrical power company of Goiás State, Brazil, were collected from March to September 2012. During this period, relative air humidity levels were very low (below 30%). Oil samples were collected across the state, according to quality control criteria based on historical series of physicochemical and chromatographic analyses from all substations. Transformers presented a wide variety of conditions, with their lifetimes ranging from one to thirty years. Samples' water/oil interfacial tension was measured via a torsion Krüss K8 tensiometer, in accordance with Brazilian technical norm ABNT NBR 6234 [28]. Oil quality is in accordance with Brazilian oil agency ANP and is regulated by technical norm ABNT NBR 10576 [29]. According to this norm, the lowest limits for interfacial tension are 22 mN m^{-1} for transformers rated below 242 kV and 25 mN m^{-1} for those rated above this voltage. In general, mineral oil samples with an interfacial tension over 35 mN m^{-1} presented excellent conditions. Those with an interfacial tension ranging from 35 to 22 mN m^{-1} are characterized as medium-quality oils, and those with an interfacial tension below 22 mN m^{-1} are considered aged. Oil in such conditions tends to form sludge, reducing circulation inside the power transformer, and the presence of water increases cellulose degradation. The color parameter was measured by a Lovibond colorimeter, according to technical norm ABNT NBR 14483 [30]. Interfacial tension values for the samples ranged from 17 to 46 mN m^{-1}, and color values ranged from 0.5 to 6.0 in dimensionless units.

2.3. Instrumentation

NIR spectra of oil samples were obtained using an FT-NIR spectrometer (Perkin Elmer Spectrum, 100N, Shelton, USA) with a transflectance accessory. Each spectrum was measured from 830 to 2500 nm with a resolution of 4 cm^{-1} and 64 scans. Fluorescence spectra were obtained by a Varian Cary Eclipse spectrofluorimeter (Palo Alto, USA), using a 10.00 mm quartz cuvette. All 2D (excitation-emission) fluorescence spectra were obtained in the 250–650 nm (10 nm steps) excitation range and in the 270–700 nm (2 nm steps) emission range. Excitation and emission monochromator slit widths were 5.0 and 2.5 nm, respectively, and the scanning rate was 9600 nm min^{-1}. ^{1}H NMR analyses were performed on a Bruker Avance III 11.75 T spectrometer at 298.0 K using a 5 mm triple-resonance broadband inverse probehead equipped with a gradient. NMR spectra were obtained at 500.13 MHz for ^{1}H, using 200 μL $CDCl_3$ and TMS in a stem coaxial insert tube used for external referencing and locking. For each determination, 240 μL of mineral insulating oil samples and 32 scans were employed. Furfural 98%, 5-Methylfurfural 98%, and 2-acetylfuran 99% were purchased from Sigma.

2.4. Data analysis

Data analysis was performed using MATLAB 7.12 (The MathWorks Natick, USA) and PLS Toolbox 6.2 (Eigenvector Research Inc., Manson, USA). In an initial stage, fluorescence, NIR, and ^{1}H NMR spectra were preprocessed separately. NIR spectra were preprocessed using baseline correction [31], multiple scattering correction (MSC), and Savitzky-Golay smoothing filter [32] with a window width of 27 points and second-order polynomial fit. A 1330–1530 nm (1 nm steps) spectral range followed variable selection of the original data ranging from 830 to 2500 nm,

totaling 201 variables. NIR spectra for all oil samples following preprocessing are shown in Fig. 1.

^{1}H NMR spectra were preprocessed using wavelet transform-assisted signal compression. This preprocessing uses a decomposition algorithm to obtain wavelet coefficients, suppressing the ones that are too small to be significant according to a threshold value. These wavelet coefficients can then be used in a wavelet series to form a family of orthonormal bases. Wavelet transforms are generally used in spectral data for compression and noise filtering. More detailed descriptions of wavelet transforms can be found in the literature [33,34]. The present work tested different families of orthogonal wavelet bases with varying orders, such as Daubechies, Symmlet, and Coiflet. Results obtained with the Symmlet family were more satisfactory according to the prediction rate criterion. This family was selected as the mother wavelet to compress the ^{1}H NMR data from 3500 to 876 variables. Savitzky-Golay smoothing filters were applied, with a window width of 15 points and second-order polynomial fit, and baseline correction [31] were performed. Peak shifts were corrected using an icoshift alignment [35] and spectra were then normalized to unit length.

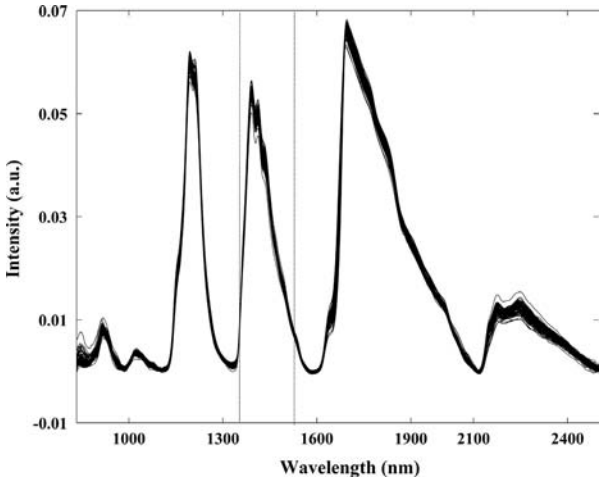

Fig. 1. NIR spectra for 100 insulating oil samples after preprocessing. Vertical lines correspond to the selected spectral range (1330–1530 nm).

Fluorescence spectra were preprocessed to remove Rayleigh and Raman scattering [36], and models were obtained following mean-centering of the original spectra.

Spectral data were split into two sets, one of 70 samples for the calibration set and another of 30 samples for the validation set, using the Kennard-Stone algorithm [37]. The best latent variables (LV) were selected according to results obtained by contiguous blocks cross-validation for all models.

3. Results and discussion

PLS2 calibration models for predicting interfacial tension and color showed an improved performance when compared to results obtained by PLS1 algorithms, owing both to the correlation between interfacial tension and color (r^2=0.6828) and to the use of physicochemical parameters instead of analyte concentrations as dependent variables. PLS2 models were generated separately for each spectroscopic data set and subsequently for the fused data set. These parameters were measured without replicates by CELG D's Insulating Materials Laboratory. Reference methods present low precision and interfacial tension values were obtained with only one significant digit.

3.1. NIR PLS model

Based on the observation of the preprocessed NIR spectra (Fig. 1), a preliminary variable selection was performed by comparing local models generated for regions around each band (873–983, 1133–1833, 1653–1833, and 2133–2433 nm) and a model was built with the whole spectra. The best PLS model was obtained in the 1330–1530 nm range, a region which corresponds to the first overtones of O–H stretching and C–H combinations. These spectral bands can be attributed [38] to cellulose and to some of its degradation products, i.e. water and furanic compounds. Water accelerates the cellulose degradation process and is an important monitoring variable of the insulating system.

Table 1 shows root mean square errors of calibration (RMSEC) and prediction (RMSEP), relative error ranges for individual samples (Range, between 0 and ±1), relative errors (RE, %), range error ratios (RER), the number of LVs, the bias, residual prediction deviation (RPD) for calibration and prediction, and correlation

Table 1
PLS2 models for NIR, ^{1}H NMR, Fluorescence, and Fused data.

	NIR	NMR	Interfacial tension[a] Fluorescence excitation[b]			Fused data		NIR	NMR	Color[d] Fluorescence excitation			Fused data	
			350	550	Fused[c]	Full	VIP			350	550	Fused	Full	VIP
RMSEC	3.9	4.3	5.2	3.4	3.7	3.2	2.9	0.6	0.6	0.7	0.4	0.4	0.4	0.3
RMSEP	4.0	5.2	5.2	3.4	3.7	3.2	2.9	0.7	0.6	0.7	0.5	0.4	0.4	0.3
Range[e]	−0.3–0.2	−0.3–0.4	−0.2–0.4	−0.2–0.4	−0.2–0.2	−0.2–0.2	−0.1–0.1	−0.2–0.4	−0.6–0.8	−0.1–0.4	−0.3–0.2	−0.3–0.2	−0.4–0.3	−0.2–0.2
RE[f] (%)	11.2	16	15.3	9.6	10.8	8.8	7.6	35	30	35	25	18	20	18
RER[g]	6.4	5.4	5.8	7.5	8.7	9.2	10.0	7.1	7.8	7.2	10.7	12.8	14.0	16.0
LV	5	4	5	5	4	4	3	5	5	5	4	2	4	3
bias	−0.752	1.108	−2.878	−0.651	−2.390	−1.499	−1.016	−0.080	−0.018	0.107	−0.170	−0.120	−0.098	−0.114
RPD[h]$_{cal}$	1.7	1.6	1.3	1.9	2.2	2.1	2.6	1.2	1.4	1.5	2.3	2.7	2.8	3.0
RPD$_{pred}$	1.4	1.2	1.1	1.6	1.5	1.8	2.1	1.2	1.5	1.3	2.0	2.4	2.6	2.9
r_{pred}	0.7200	0.8333	0.6976	0.8011	0.8645	0.8797	0.8956	0.6803	0.7384	0.6928	0.8739	0.9353	0.9399	0.9538

[a] mN m^{-1}.
[b] nm.
[c] 350+550.
[d] dimensionless unit.
[e] Range of relative errors for individual samples (between −1 and 1).
[f] Mean Relative Error.
[g] Range error ratio.
[h] Residual prediction deviation.

coefficient rpred between reference and predicted values for this model. The low and comparable RMSEC and RMSEP values for both parameters, together with the low number of LVs, indicate that models were not overfitted. In general, the figures of merit values for interfacial tension prediction are better than the ones for color prediction. RMSEP, RMSEC, and the relative errors of prediction for individual samples are parameters for evaluating the accuracy of the models. NIR models provided a reasonable RMSEP of 4.0 mN m^{-1} and a mean relative error of prediction of 11.2% for interfacial tension, as well as an RMSEP of 0.7 mN m^{-1} and a high mean relative error of 35% for color. Correlation coefficients of 0.7200 and 0.6803 indicated that both models did not present good linearities. The bias was estimated only with validation samples to verify the presence of systematic errors in the model [40]. The estimated bias of -0.752 mN m^{-1} and -0.080 were used jointly with their standard deviations of validation errors (5.8 mN m^{-1} and 1.0) in two-tailed *t*-tests with 29 degrees of freedom ($t_{tab}=2.045$, $P=0.05$), which indicated the absence of statistically significant bias only for color. RPD and RER are parameters proposed for assessing the predictive ability of multivariate calibration models in absolute terms, regardless of the analytical ranges [41]. RPD, the ratio of standard deviations of the reference values for prediction errors (RMSECV for calibration and RMSEP for prediction) is more often used, but RER, the ratio of the analytical ranges for prediction errors, is considered more sensitive to determine a model's practical utility [42]. RPD values higher than 2.4 are considered desirable for good calibration equations, whereas values lower than 1.5 are considered unusable [41]. Thus, RPD_{pred} values of 1.4 and 1.2 for interfacial tension and color, respectively, pointed to the limited quality of the NIR models proposed.

3.2. ^{1}H NMR PLS model

^{1}H NMR 7.40–6.40 ppm (0.0003 ppm steps) spectral region was used for building the PLS model. In this spectral range, chemical shifts of hydrogens attached to furanic compounds such as 2-furaldehyde, 5-hydroxymethyl-2-furaldehyde, and furfuryl alcohol were observed. The 7.40–6.40 ppm region of the ^{1}H NMR average spectrum of the 100 mineral oil samples analyzed and the chemical structures for three of the furanic compounds formed during the degradation of the insulating system are shown in Fig. 2. Peaks for the chemical shifts of protons of the three out of five furanic compounds found in degraded mineral oils can be observed. Chemical shifts already assigned to aromatic hydrogens

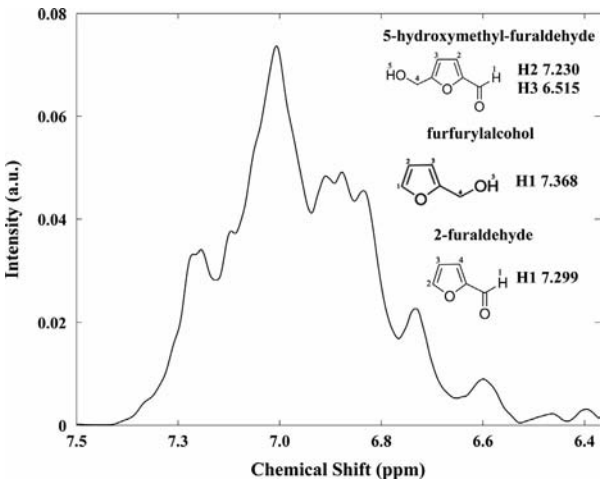

Fig. 2. The 7.4–6.4 ppm region of the ^{1}H NMR average spectrum of 100 mineral oil samples. Assignment regions for three furanic compounds are also shown.

were collected from the website of Spectral Database for Organic Compounds (SDBS) [39]. Results obtained for PLS models built with NMR data, shown in Table 1, are similar to NIR models as regards color prediction, but proved worse for interfacial tension prediction. Thus, these models showed a limited quality.

3.3. Fluorescence PLS models

Two excitation wavelengths were selected at 350 and 550 nm, and two emission spectra ranges from 300 to 500 nm, and from 508 to 700 nm, respectively. Emission spectra at the two excitation wavelengths were analyzed separately and jointly, totaling 196 variables for the fused data. According to the contour maps shown in Fig. 3, it is possible to infer that during the ageing process a drastic change in the fluorescence spectra occurs, caused by the degradation of some oil constituents and the formation of new fluorophores. Non-degraded oil samples have high interfacial tension and emit excitation wavelengths ranging from 350 to 370 nm, with two peaks of maximum fluorescence (emission) intensities at 380 and 400 nm (Fig. 3A). On the other hand, a degraded sample (low interfacial tension) emits excitation wavelengths ranging from 450 to 650 nm and presents a peak of maximum fluorescence intensity at approximately 520 nm (Fig. 3B). The fluorescence plot of 5-methyl-2-furfural, which is one of the aromatic compounds known to be produced during cellulose degradation, is shown in Fig. 3C. Both excitation and emission ranges for this compound corresponded well to the same ranges of an aged sample. It is important to stress that, of the three furanic compounds shown in Fig. 2, 5-methyl-2-furfural has the highest fluorescence intensity, as can be seen in Fig. 4.

PLS models were built for excitation wavelengths of 350 nm (maximum excitation wavelength of brand new samples), 550 nm (maximum excitation wavelength of aged samples), and 350+550 nm (fused excitation fluorescence). Models were obtained by four LVs and are presented in Table 1. The best model for both parameters was obtained from the fused spectra collected in both excitation wavelengths. These models presented RMSEP values of 3.7 mN m^{-1} for interfacial tension and 0.4 for color, which are lower than the ones obtained with NIR and NMR. They also provided higher values of RPD, RER, and correlation coefficients. These results indicate that fluorescence data may be more specific for evaluating insulating oil quality due to the emission of furanic compounds, which are specific degradation products of the system. Parallel Factor Analysis (PARAFAC) and N-way PLS as second-order calibration models were also generated, but their prediction errors were higher than the ones obtained from ordinary PLS and data fusion.

3.4. Data fusion

The row-wise augmented data matrix formed by the fusion of fluorescence (350 and 550 nm emissions), NIR, and ^{1}H NMR spectral data, totaling 1276 variables, was auto-scaled (mean-centering plus equal variance scaling) to give equal weights to the spectra obtained from techniques of different natures. In Fig. 5, these four spectral data sets were plotted before being fused into a single one. PLS models built with the full meta-spectra were obtained from four and two LVs for interfacial tension and color models, respectively, as shown in Table 1. To improve model prediction, an optimal spectral selection of variables was attempted using VIP scores. A total of 291 out of 1276 variables was selected for the final PLS model according to the criterion of VIP score values greater than 1. More than half of the variables were selected from the spectrofluorimetric data.

The best PLS model for predicting interfacial tension was obtained by using three LVs. 77.60% of accumulated variance of

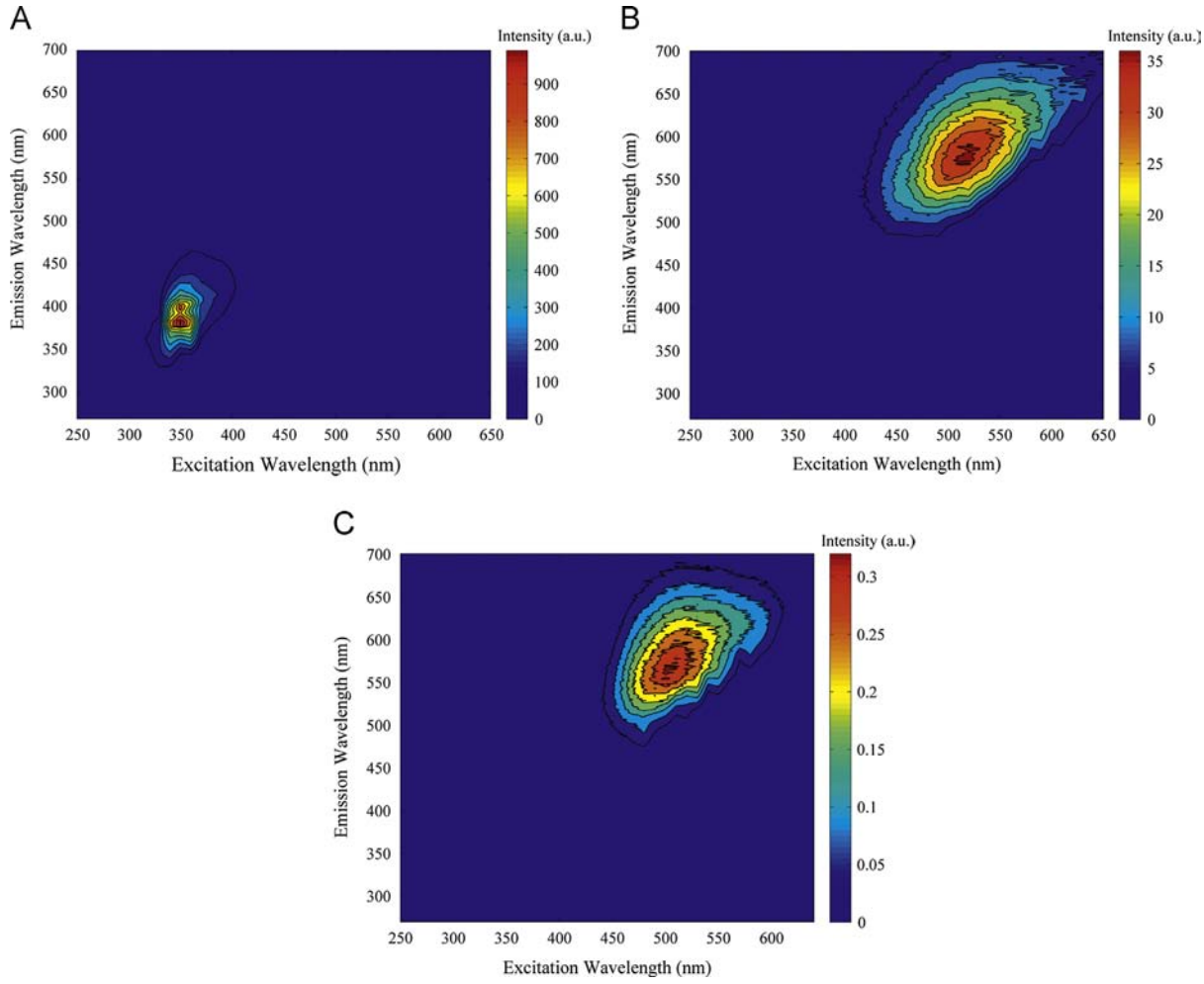

Fig. 3. Fluorescence excitation-emission contour maps of a non-degraded sample with a 42 mN m^{-1} interfacial tension (A); a degraded sample with a 17 mN m^{-1} interfacial tension (B); 5-methyl-2-furfural (C).

the X data matrix and 87.54% of the Y data matrix were accounted for in this model. When all variables (full model) were included in the regression model, percentages reached 93.39% and 85.47% for X and Y data matrices, respectively. For color prediction, the best PLS model was also obtained with three LVs and accounted for 81.01% of accumulated X variance and 91.39% of Y variance. For the full model, percentages were 87.09% and 88.74% for X and Y matrices, respectively. Correlation plots between predicted versus experimental values for both interfacial tension and color are presented in Fig. 6; they provided the best linear models, with coefficients of 0.8956 and 0.9538, respectively. In conclusion, data fusion models using VIP-score variable selection were the most effective ones. The prediction errors for color were slightly lower than the ones provided by fluorescence fused spectra. On the other hand, this model had the lowest errors among all the tested models when predicting interfacial tension, with RMSEC and RMSEP both equal to 2.9 mN m^{-1}. These values were similar to those obtained previously with multi-way calibration models and image analysis for insulating oil samples [43].

RER, RPD, and bias were also used as performance criteria for PLS models, as shown in Table 1. RPD values varied from 1.0 to 2.0 for non-fused models and from 2.0 to 3.0 for fused models using VIP scores. The best RPD results for fused data models, most of them above 2.4 [41], seem to indicate better predictive ability when compared to non-fused data. Estimates using two-tailed t test, $p=0.05$, revealed that models were not subject to systematic bias. Table 1 also presents RER values calculated for all PLS models. RER values ranged from 5.4 for PLS-NMR to 16.0 for PLS-VIP fused data. RER values between 3 and 10 show limited to good practical utility, whereas values above 10 show that the model has high utility [42]. Therefore, fused models provided the highest RER values, thus confirming their greater predictive quality. Non-linear Support Vector Regression models (SVR-VIP) were also tested, but they did not help improve results obtained by PLS (in both cases using VIPs).

Even though PLS regression models obtained from data fusion of all spectroscopic variables provided the lowest prediction errors for interfacial tension, it was also possible to predict the parameters with rather low errors using any of the three spectroscopic techniques individually. Among the techniques tested, fluorescence was considered the most effective in evaluating the quality of insulating oils and in identifying degraded samples through EEM surfaces.

4. Conclusions

The combined use of NIR, fluorescence, and NMR, together with low-level data fusion and VIP-score variable selection, provided optimal multivariate calibration models for interfacial tension prediction and for power transformers' insulating oil quality evaluation. Discrimination between degraded (aged) and non-degraded (new) samples is possible using this approach. Fluorescence was found to be the best individual technique for predicting

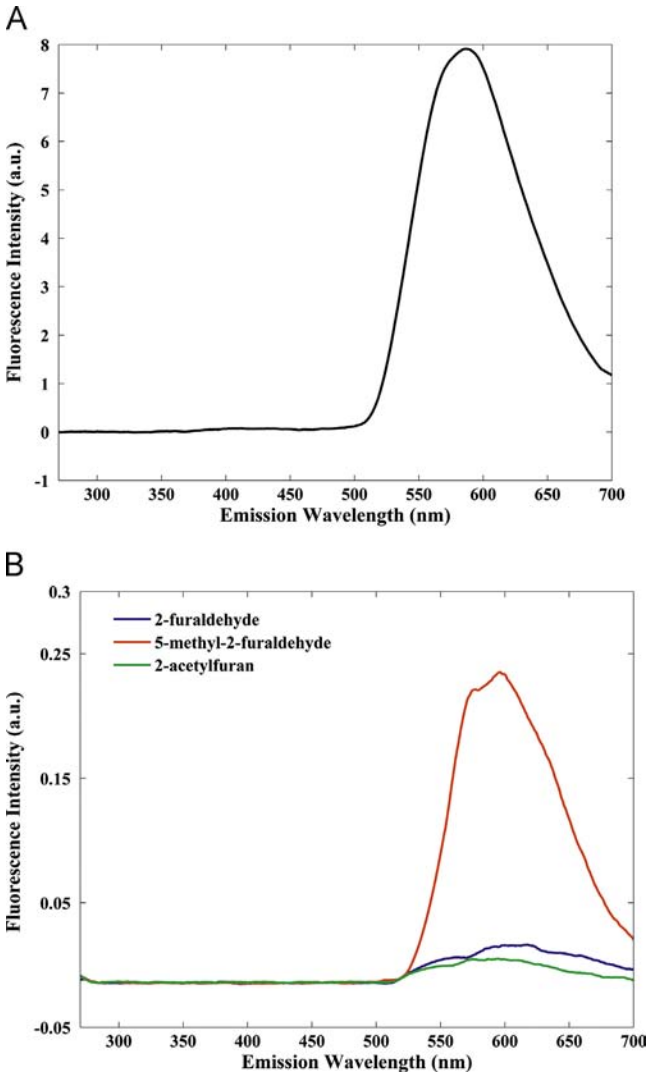

Fig. 4. Fluorescence emission spectra at 550 nm of excitation: degraded oil sample (A); three furanic compounds commonly found in degraded oil samples (B).

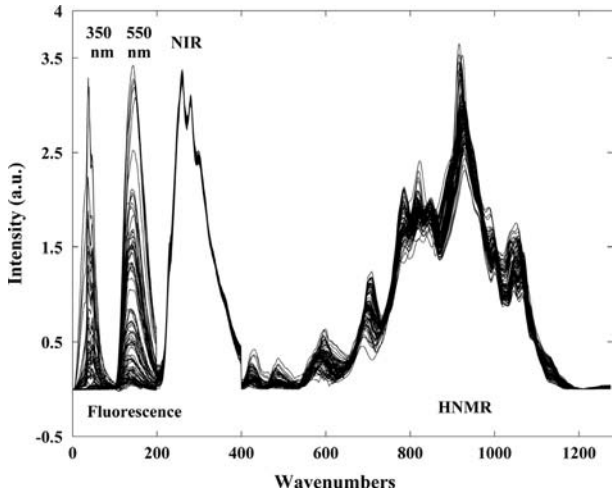

Fig. 5. Meta-spectra obtained by fusing fluorescence (350 and 550 nm emissions), NIR, and ^{1}H NMR data.

interfacial tension, since it is direct, rapid, non-destructive, and environmentally friendly (does not generate any chemical residues). Finally, this work opens perspectives for a possible implementation

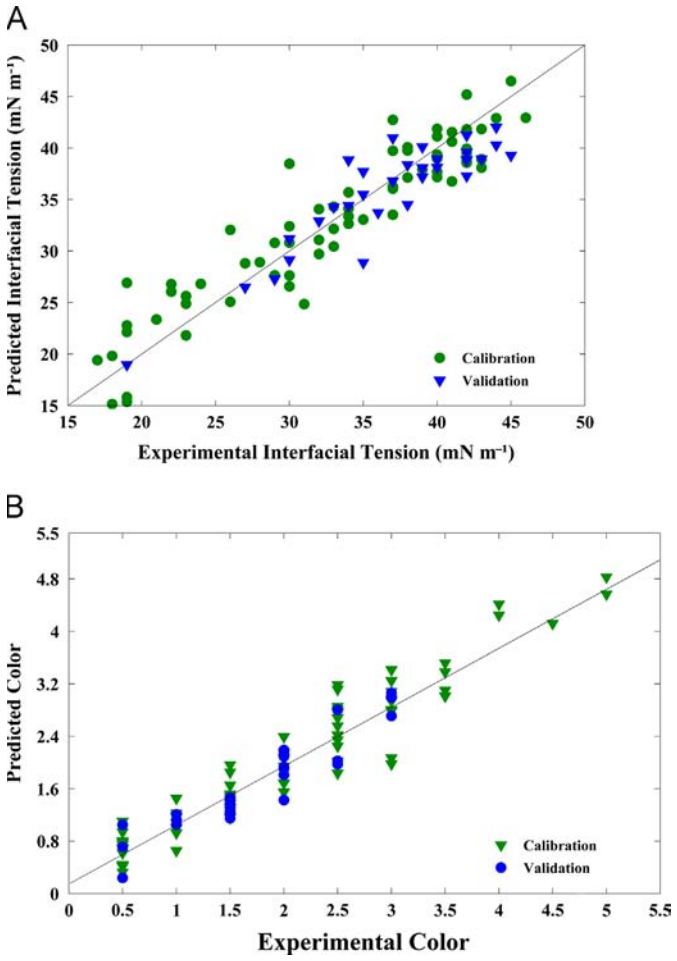

Fig. 6. PLS predicted versus reference values for interfacial tension (A) and color (B) for VIP-score data fusion model. Calibration and validation sets.

of non-invasive, on-line assessment of ageing conditions of power transformers' insulating systems through the use of multivariate sensors, which can be based on different spectroscopic techniques.

Acknowledgment

Financial support from Conselho Nacional de Pesquisa (CNPq) (Grant no. 554603/2010-1) is gratefully acknowledged. M.S.G. thanks CNPq and "Ciência sem Fronteiras" program for a Ph.D. fellowship. The authors also thank CELG D and IDAEA-CSIC.

References

[1] T.O. Rouse, IEEE Electr. Insul. M. 14 (1998) 6–16.
[2] P. Verma, M. Roy, R.K. Tiwari, S. Chandra, Electr. Insul. Conf. Electr. Manuf. 1 (2005) 112–116.
[3] A.J. Kachler, I. Hohlein, IEEE Electr. Insul. M. 21 (2005) 15–21.
[4] A.M. Emsley, G.C. Stevens, IEEE Proc.Sci. Meas. Technol. 141 (1994) 324–334.
[5] R. Phadungthin, E. Chaidee, J. Haema, T. Suwanasri, Electr. Eng./Electr. Comput. Telecommun. Inf. Technol. (ECTI-CON) Conf. 1 (2010) 108–111.
[6] M.S. Godinho, A.E. de Oliveira, M.M. Sena, J. Near Infrared Spectrosc. 19 (2011) 243–251.
[7] ASTM D1500-12, Standard test method for ASTM color of petroleum products (ASTM color scale), American Society for Testing and Materials, West Conshohocken, PA, USA, 2012.
[8] T.K. Saha, IEEE Trans. Dielectr. Electr. Insul. 10 (2003) 903–917.
[9] J.P. van Bolhuis, E. Gulski, J.J. Smit, IEEE Trans. Power Deliv. 17 (2002) 528–536.
[10] ASTM D5837-12, Standard test method for furanic compounds in electrical insulating liquids by High-Performance Liquid Chromatography (HPLC), American Society for Testing and Materials, West Conshohocken, PA, USA, 2012.

[11] S. Das, A.M. Powe, G.A. Baker, B. Valle, B. El-Zahab, H.O. Sintim, M. Lowry, S.O. Fakayode, M.E. McCarroll, G. Patonay, M. Li, R.M. Strongin, M.L. Geng, I.M. Warner, Anal. Chem. 84 (2012) 597–625.
[12] M.R. Monteiro, A.R.P. Ambrozin, M.S. Santos, E.F. Boffo, E.R. Pereira-Filho, L.M. Lião, A.G. Ferreira, Talanta 78 (2009) 660–664.
[13] L. Vera, L. Aceña, J. Guasch, R. Boqué, M. Mestres, O. Busto, Talanta 87 (2011) 136–142.
[14] M. Brady, Foreword, Int. J. Robot. Res. 7 (1988) 2–4.
[15] M. Casale, C. Casolino, P. Olivieri, M. Forina, Food Chem. 118 (2010) 163–170.
[16] M. Casale, P. Olivieri, C. Casolino, N. Sinelli, P. Zunin, C. Armanino, M. Forina, S. Lanteri, Anal. Chim. Acta 712 (2012) 56–63.
[17] C. Pizarro, S. Rodríguez-Tecedor, N. Pérez-del-Notario, I. Esteban-Díez, J.M. González-Sáiz, Food Chem. 138 (2013) 915–922.
[18] D. Cozzolino, H.E. Smyth, K.A. Lattey, W. Cynkar, L. Janik, R.G. Dambergs, I.L. Francis, M. Gishen, Anal. Chim. Acta 563 (2006) 319–324.
[19] C.V. Di Anibal, M.P. Callao, I. Ruisánchez, Talanta 84 (2011) 829–833.
[20] C. Alamprese, M. Casale, N. Sinelli, S. Lanteri, E. Casiraghi, LWT – Food Sci. Technol. 53 (2013) 225–232.
[21] P.M. Ramos, I. Ruisánchez, K.S. Andrikopoulos, Talanta 75 (2008) 926–936.
[22] M.A. Solano, S. Ekwaro-Osire, M.M. Tanik, Inf. Fusion 13 (2012) 79–98.
[23] T.G. Doeswijk, A.K. Smilde, J.A. Hageman, J.A. Westerhuis, F.A. van Eeuwijk, Anal. Chim. Acta 705 (2011) 41–47.
[24] S. Wold, E. Johansson, M. Cocchi, PLS – partial least squares projections to latent structures, in: H. Kubinyi (Ed.), 3D-QSAR in Drug Design: Theory, Methods and Applications, vol. 1, Kluwer Academic Publishers, Dordrecht, 1993, pp. 523–550.
[25] I. Chong, C. Jun, Chemom. Intell. Lab. Syst. 78 (2005) 103–112.
[26] H.H. Zhang, Variable selection methods: an introduction, University of Arizona, ⟨http://math.arizona.edu/~hzhang/waeso/vsTutorial.pdf⟩ (accessed on 10.01.13).
[27] S. Wold, M. Sjostrom, L. Eriksson, Chemom. Intell. Lab. Syst. 58 (2001) 109–130.
[28] ABNT NBR 6234, Método de ensaio para a determinação de tensão interfacial de óleo-água, Associação Brasileira de Normas Técnicas, São Paulo, Brazil, 1965.
[29] ABNT NBR 10576, Óleo mineral isolante de equipamentos elétricos – Diretrizes para supervisão e manutenção, Associação Brasileira de Normas Técnicas, São Paulo, Brazil, 2006.
[30] ABNT NBR 14483, Produtos de petróleo – determinação da cor – método do colorímetro ASTM, Associação Brasileira de Normas Técnicas, São Paulo, Brazil, 2005.
[31] H.F.M. Boelens, P.H.C. Eilers, T. Hankemeler, Anal. Chem. 77 (2005) 7998–8007.
[32] A. Savitzky, M.J.E. Golay, Anal. Chem. 36 (1964) 1627–1639.
[33] X. Shao, A.K. Leung, F. Chau, Acc. Chem. Res. 36 (2003) 276–283.
[34] M. Vannucci, F. Corradi, J. R. Statist. Soc. B 61 (1999) 971–986.
[35] F. Savorani, G. Tomasi, S.B. Engelsen, J. Magn. Reson. 202 (2010) 190–202.
[36] M. Bahram, R. Bro, C. Stedmon, A. Afkhami, J. Chemometr. 20 (2006) 99–105.
[37] R.W. Kennard, L.A. Stone, Technometrics 11 (1969) 137–148.
[38] J.S. Shenk, J.J. Workman Jr., M.O. Westerhaus, Application of NIR spectroscopy to agricultural products, in: D.A. Burns, E.W. Ciurczak (Eds.), Handbook of Near-Infrared Analysis, 3rd Ed.,CRC Press, New York, 2008, pp. 347–387.
[39] National Institute of Advanced Industrial Science and Technology (AIST), Spectral Database for Organic Compounds (SDBS), Japan, ⟨http://sdbs.riodb.aist.go.jp/sdbs/cgi-bin/cre_index.cgi⟩ (accessed on 10.01.13).
[40] ASTM, E1665-05, Standard practices for Infrared multivariate quantitative analysis, American Society for Testing and Materials, West Conshohocken, PA, USA, 2012.
[41] P.C. Williams, Variables affecting near-infrared reflectance spectroscopy analysis, in: P. William, K. Norris (Eds.), Near-Infrared technology in the agricultural and food industries, American Association of Cereal Chemists Inc1987, pp. 143–167.
[42] C.C. Fagan, C. Everard, C.P. O'Donnell, G. Downey, E.M. Sheehan, C.M. Delahunty, D.J. O'Callaghan, J. Dairy Sci. 90 (2007) 1122–1132.
[43] M.S. Godinho, A.E. Oliveira, M.M. Sena, Microchem. J. 96 (2010) 42–45.